

The Tensile Properties of Pearlite, Bainite, and Spheroidite

M. Gensamer · E. B. Pearsall · W. S. Pellini ·
J. R. Low Jr.

© American Society for Metals 1942

Abstract The tensile properties of four steels have been determined as a quantitative function of the measured dimensions of the aggregate structures pearlite and spheroidite, and of the austenite decomposition temperature for the structures pearlite and bainite. Studies of the recalescence effect have been performed in connection with the measurement of the reaction temperature. The strength indices (stress at corresponding strains, tensile strength, hardness) vary linearly with the reaction temperature and the logarithm of the dimensions of the aggregate. Mixtures of pearlite and bainite are intermediate in strength. The ductility indices are low for mixed structures, coarse pearlite and low temperature bainite; higher for bainite and pearlite in the middle of the reaction temperature range for each. It has been observed that spheroidized eutectoid specimens have a typical mild steel yield point; pearlitic specimens of the same tensile strength do not. The spacing of pearlite is shown to be proportional to the carbon diffusion coefficient in austenite, the logarithm of the spacing plotting as a straight line against the reciprocal of the absolute reaction temperature, with the same slope as a similar plot for the diffusion coefficient. Because of this it is concluded that a measurement of the spacing at one temperature permits its calculation at another,

using the measured energy of activation for the diffusion of carbon in the steel. A rule of strength for aggregates is proposed, based on these studies, as follows: The resistance to deformation of a metallic aggregate consisting of a hard phase dispersed in a softer one is proportional to the logarithm of the mean straight path through the continuous phase. The rule works for a comparison of the properties of pearlite and spheroidite, as well as for pearlite alone over a wide range of spacings, and extrapolates to reasonable particle sizes for the finest spheroidites (tempered martensite). A simple explanation of the semilogarithmic character of the relationship is advanced.

Keywords Microstructure · Tensile properties · Mechanical properties · Pearlite · Bainite

This paper is the second of a series dealing with the quantitative correlation of the microstructures observed in metals and alloys with the mechanical properties of these structures. It deals with the mechanical properties of structures consisting of a hard phase dispersed in a soft one, and particularly with those aggregate structures in steel known as pearlite, spheroidite, and bainite. The structure of pearlite is lamellar; the particles in spheroidite are approximately spheroidal, while the fine structure of bainite is still uncertain. Work on the specific effect of various alloying elements in solution in ferrite is in progress, and work on the effect of grain size on the properties of ferrite will be reported in the near future. It is hoped that these studies will help in the development of a theory of the strength of metals and alloys, and perhaps be of use in their practical utilization.

Two years ago Gensamer et al. [1] presented what was intended to be a study of the mechanical properties of a

Reprinted from *Transactions of American Society for Metals*, Vol. 30, December 1942, 983–1019, Copyright American Society for Metals.

A paper presented before the Twenty-third Annual Convention of the Society held in Philadelphia, October 20–24, 1941. At the time of original publication, the authors were all associated with the Metals Research Laboratory at the Carnegie Institute of Technology, Pittsburgh. M. Gensamer was also associate professor of metallurgy there, and J. R. Low, Jr., was the Carnegie-Illinois Steel Company Graduate Fellow in Metallurgical Engineering. Manuscript received June 23, 1941.

plain carbon (eutectoid) steel reacted isothermally at temperatures from 375 to 750 °C (705 to 1380 °F), in which will be found a list of references to previous work on the subject. In the discussion of that paper the authors pointed out that the reaction temperatures reported were in error because of recalescence during the reaction, and that the results would need to be corrected for this error. The conclusion reached without this correction that the mechanical properties plot as straight lines against the reaction temperature over the whole range from 375 to 700 °C (705 to 1290 °F) (in the bainite range as well as the pearlite range) must be abandoned, as well as certain speculations concerning the nature of bainite based on this conclusion. The primary purpose of that research, namely, to correlate properties with the interlamellar spacing of pearlite, is in no way affected by this correction.

The present paper extends the knowledge of the properties of these reaction products. The actual reaction temperature ranges have been determined for the steel of the earlier paper, enabling a replotting of the data, now against true reaction temperature. In addition, a large number of tests have been performed on another heat of rope wire steel of almost the same analysis from a different producer. The results with the two steels are in good agreement. It was decided not to continue with the fatigue strength determinations, for in the earlier tests all the fatigue strength values were between 50 and 55% of the tensile strength.

The present paper reports also on the properties of the second steel after spheroidization of the cementite, and the correlation of the spheroidal and lamellar structures in the same steel. This has resulted in a general theory of strength for metallic aggregates, the most important contribution of the second paper.

Tests have also been made on two manganese steels of approximately eutectoid carbon content. The first of these, with 0.56% carbon and 1.50% manganese, is slightly hypoeutectoid. It is a high manganese rail steel; samples were cut from a rail, using only metal from the top surface of the head and the bottom surface of the base, to avoid ingot segregation. The actual reaction temperature for this steel was never much more than 20° above the bath

temperature, and most of the reaction certainly occurred not more than 10 °C (18 °F) from the bath temperature. The second alloy steel, with 0.56% carbon and 3.5% manganese, is very close to the eutectoid composition. It is a small induction furnace heat made by experienced melters. This steel reacted very slowly and so without detectable recalescence and wholly at the bath temperature.

The results with the rail steel were quite similar to those with the lower manganese rope wire steel, but the quantitative correlation of properties with pearlite spacings was not accomplished with this steel, mainly because the temperature range in which only pearlite is formed seems to be quite narrow. There is considerable doubt that the reaction product is entirely pearlite except at the highest reaction temperatures, and there the time of reaction is so long as to make spheroidization of a fair amount of pearlite probable. The 3.5% manganese steel apparently forms only pearlite over a wider temperature range, but in this steel the pearlite is ill-formed and perhaps spheroidized to a considerable extent, so that the correlation of properties with pearlite spacing may be only qualitative.

Materials and Heat Treatment

Steels A and B (low manganese) were used without homogenization prior to the austenitizing treatment (Table 1). They were obtained as single bundles of 3/8-inch diameter hot rolled rods, from which the specimens were machined; there has been no evidence for segregation in these steels after the austenitizing treatment, either in rate of reaction or structure. Both the manganese steels were given a homogenization treatment before the standard reaction treatment. They were both homogenized from 48 to 60 h at 1250 °C (2280 °F) in an atmosphere of argon or helium; in the helium slight surface decarburization was observed, but after machining the carbon was not appreciably lower (by analysis) than before homogenization. The rail steel was cooled with the furnace to 900 °C (1650 °F), then plunged quickly into “sil-o-cel” insulating powder. The 3.5% manganese steel was cooled with the furnace to 750 °C (1380 °F), then cooled in the sil-o-cel. The sil-o-cel

Table 1 Analysis and austenite grain size of the steels used

	Carbon	Manganese	Phosphorus	Sulfur	Silicon	Copper	Nickel	Chromium	Austenite grain size no. before quenching
Steel A	0.78	0.63	0.014	0.030	0.18	8-9
Steel B	0.80	0.74	0.019	0.029	0.24	0.09	0.11	0.01	5
Steel C	0.56	1.56	0.025	0.031	0.15	5
Steel D	0.57	3.5	0.26	5
Steel E	0.66	0.61	0/016	0.014	0.18	0.11	0.09	0.04	..

cooling was rather fast at high temperatures and thus tended to prevent the heterogeneity developed by these steels on slow cooling through the 3-phase field. On subsequent heating to the quenching temperature of 850 °C (1560 °F), both steels developed an austenite grain size of ASTM number 5, determined after reaction, and low-temperature decarburization. This homogenization eliminated the banding obtained in both steels in the forged (3.5% manganese) and rolled (1.5% manganese) condition as received.

Steel A was quenched after one-half hour in lead at 825 °C (1515 °F) (resulting in an austenite grain size number 8–9) into lead at various temperatures below the critical, held at the lower lead bath temperature (hereafter referred to as the bath temperature) for a sufficient length of time to complete the reaction (determined by pilot experiments), slowly cooled in the lead bath to a temperature near the melting point of lead and then removed from the lead and cooled in sil-o-cel to room temperature. Steels B, C, and D were quenched after one-half hour in lead at 850 °C (1560 °F) (all having an austenite grain size number 5) into lead below the critical, held to complete the reaction, then removed from the lead and either quenched in water or cooled in sil-o-cel; all specimens of Steel C were water quenched, all of Steel D were sil-o-cel cooled; some specimens of Steel B were also cooled in the lead. Cooling in the lead is very slow cooling; cooling in sil-o-cel is initially about as rapid as air cooling, but at low temperatures much slower. The plots of properties versus reaction temperature distinguish the various kinds of cooling used; it is concluded that no significant difference results from different rates of cooling following reaction except that very slow cooling (furnace cooling) gives slightly lower strengths, probably because of partial spheroidization of the reaction product.

The spheroidized structures were prepared (only for Steel B) by annealing oil-quenched specimens for appropriate lengths of time at temperatures beneath the critical. The size of the spheroids is a function of both temperature and time. A variety of treatments was tried, including attempts to produce spheroidites by direct reaction from austenite, in an effort to produce spheroidites with the best possible regularity of size of particles, but none of these experiments were successful in producing any more uniform spheroidites than simple annealing of quenched specimens.

Determination of Reaction Temperature for Lead Quenching

The actual reaction temperatures for the lead-quenched specimens were determined by inserting a thermocouple

through a small hole on the axis of a specimen of the same diameter as those heat treated for the tensile tests (0.260-inch diameter). This specimen is sketched in Fig. 1. Two fine chromel–alumel thermocouple wires (28 gage) were butt welded to the bottom of the hole. The wires were insulated with a porcelain enamel before insertion. The hole had a diameter of 0.075 inch and was therefore only 8% of the total cross section area, so that the rate of cooling at the thermocouple weld might be expected to differ little from the rate of cooling of a solid sample. To check this point, the microstructure of specimens with thermocouples was compared with the microstructure of solid tensile test specimens at important temperatures (550 and 625 °C) in both the fully reacted and partially reacted conditions; no significant differences were observed, so the authors feel confident that the cooling curves and reaction temperatures determined from them apply to the specimens used for the mechanical tests. The galvanometer used had a sufficiently low period to eliminate error from this source. As the light beam traveled over the galvanometer scale, a chronograph key was tapped at convenient temperature intervals; this provided the data for the cooling curves assembled in Fig. 2. The data plotted in Fig. 2 were determined using Steel B, but the curves apply equally well to the data for Steel A, which are not shown.

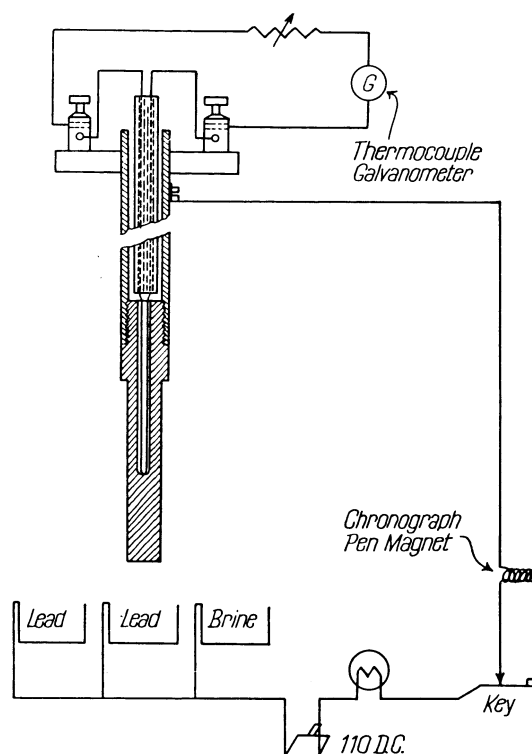


Fig. 1 Sketch of the specimen and the wiring diagram for the apparatus used in determining the reaction temperatures

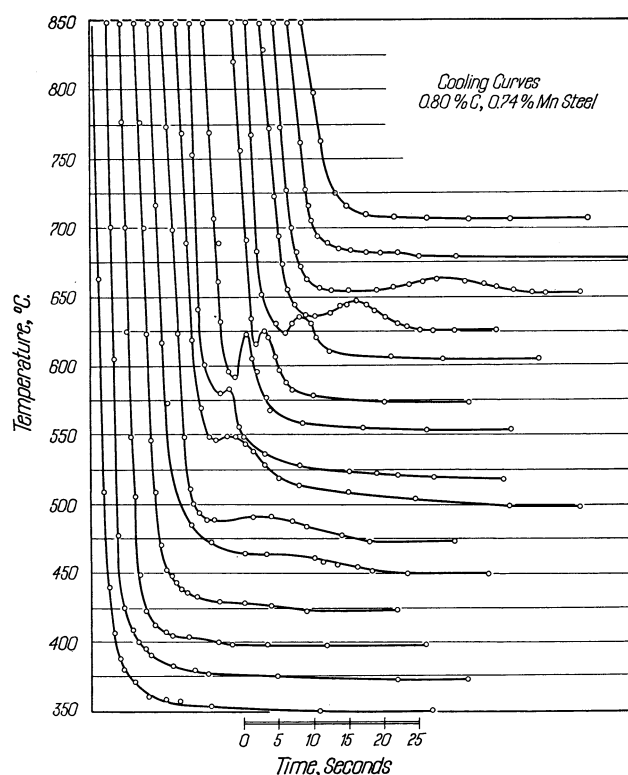


Fig. 2 Cooling curves for 0.26-inch diameter cylinders of plain carbon eutectoid steel quenched into lead baths at various temperatures

A series of experiments was performed to correlate the reaction temperature with the experimental cooling curves. The progress of cooling (and recalescence) was interrupted at various stages by a drastic quench in brine and the progress of the reaction determined from the microstructure. The cooling curve for each sample was determined to within a fraction of a second of the time of interruption of cooling and in every instance agreed very well with the uninterrupted curve, as may be seen in Figs. 3 and 4. The exact times of entry into the lead bath and of quenching into the brine were indicated on the chronograph record by having the specimen part of an electrical circuit including the chronograph key, the magnet actuating the chronograph pen, and all the baths in parallel, as in Fig. 1, so that when the sample was removed from any bath this was indicated on the chronograph record. It was observed that the temperature dropped at a very rapid rate immediately after the specimen entered the brine; the reaction may have continued for a short time after the time indicated by the chronograph upon quenching, but it must certainly have been a small fraction of a second. The temperature at the instant of quenching into the brine was not observed, but taken at the appropriate time from the cooling curve. It will be observed that the interrupted curves closely follow each other and the uninterrupted curve up to the time of interruption.

The experiments summarized in Figs. 3 and 4 show that for lead bath temperatures of 550 and 625 °C (1020 and 1155 °F) the entire reaction takes place in the temperature range between the minimum just before recalescence and the maximum reached during recalescence. The reaction is about half completed at the recalescence maximum, and as far as can be seen with the microscope, it is over by the time the temperature again falls to the minimum just before recalescence. The mean of this temperature range has been taken as the reaction temperature for the plots of properties against reaction temperature reported below. At lower bath temperatures, the reaction temperature range was estimated from the apparent disturbance of the normal, smooth cooling curve; there is some uncertainty about the lower limit of the reaction range for these temperatures, but it is so near the bath temperature that no important error can be introduced.

The reaction temperature range and the temperature chosen as the mean reaction temperature are plotted in Fig. 5 against the bath temperature. This graph applies to both Steel A and Steel B (plain carbon). Figure 6 is the same thing for Steel C (the rail steel). The 3.5% manganese steel (Steel D) showed no appreciable recalescence. Figures 5 and 6 apply to cylinders 0.260 inch in diameter with fairly vigorous hand stirring and clean lead baths with a coarse carburizing compound cover. It has been shown experimentally by a lengthy series of special tests during the progress of this work that failure to stir and dirty lead baths, and especially contamination of the carbonaceous lead bath cover by lead oxide, all lead to slow rates of cooling and higher reaction temperatures. Small specimens react nearer the bath temperature, but it seemed inadvisable to use specimens smaller than 1/4 inch diameter, which is half the size of the standard tensile specimen. One-eighth-inch diameter specimens exhibit recalescence even when using the best quenching technique, near the temperature of fastest reaction, so that their reaction temperature is above the bath temperature. Experimental cooling curves made with Steel A indicate that at 550 °C (1020 °F) (the temperature of maximum recalescence), 1/4-inch specimens react about 50° above the bath temperature, 1/8-inch specimens about 20°; these figures are for the mean temperature of the reaction and not the maximum at which the reaction occurs, which is even higher. With 0.075-inch specimens the reaction begins about 8° above the bath temperature.

Mechanical Test Results

In Figs. 7–10 are plotted the tensile properties obtained on quenching into lead baths for the four steels studied. The testing techniques and specimens are the same as those

Fig. 3 Correlation of the progress of the reaction with cooling curves for quenching into lead at 550 °C, by quenching into brine at various stages

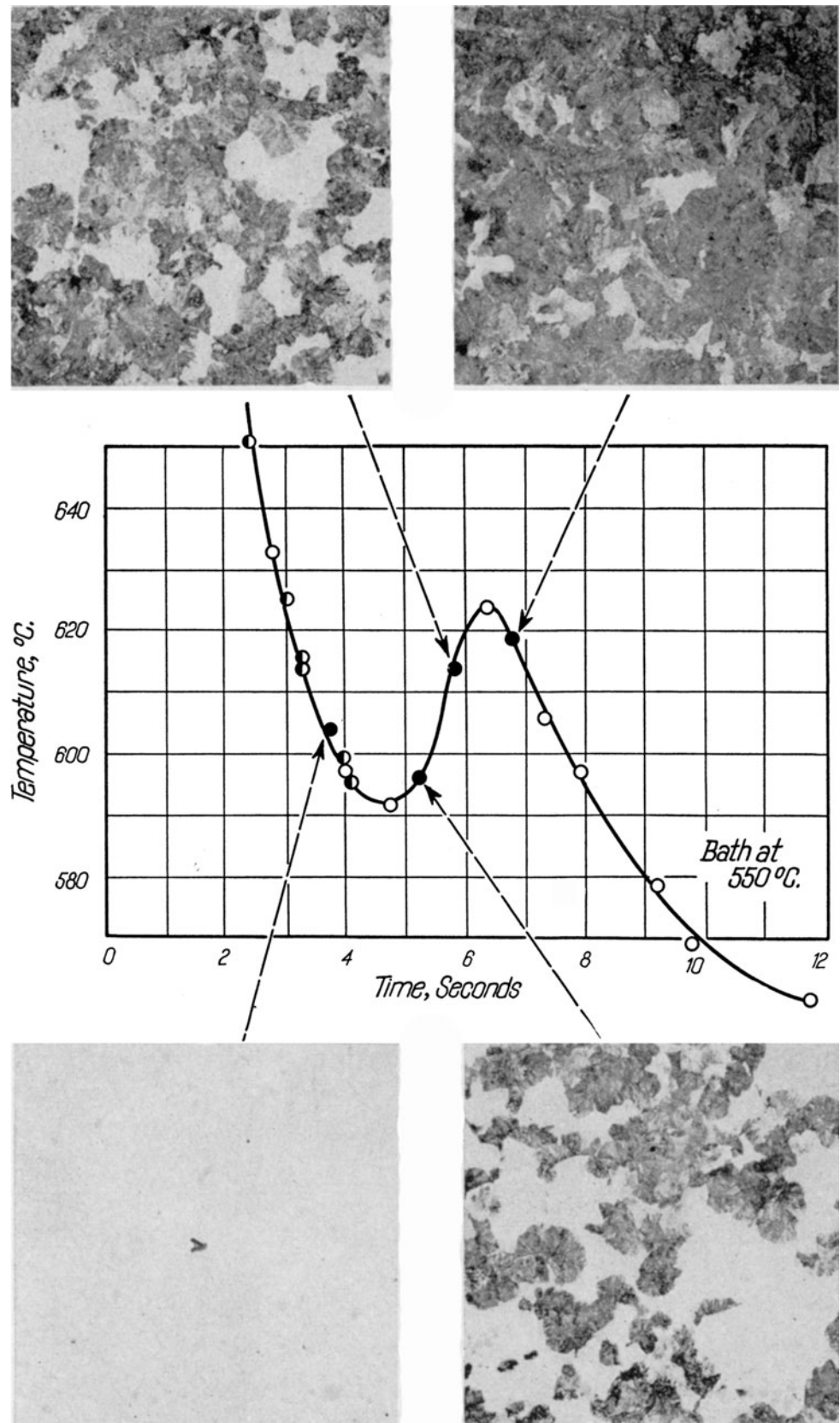
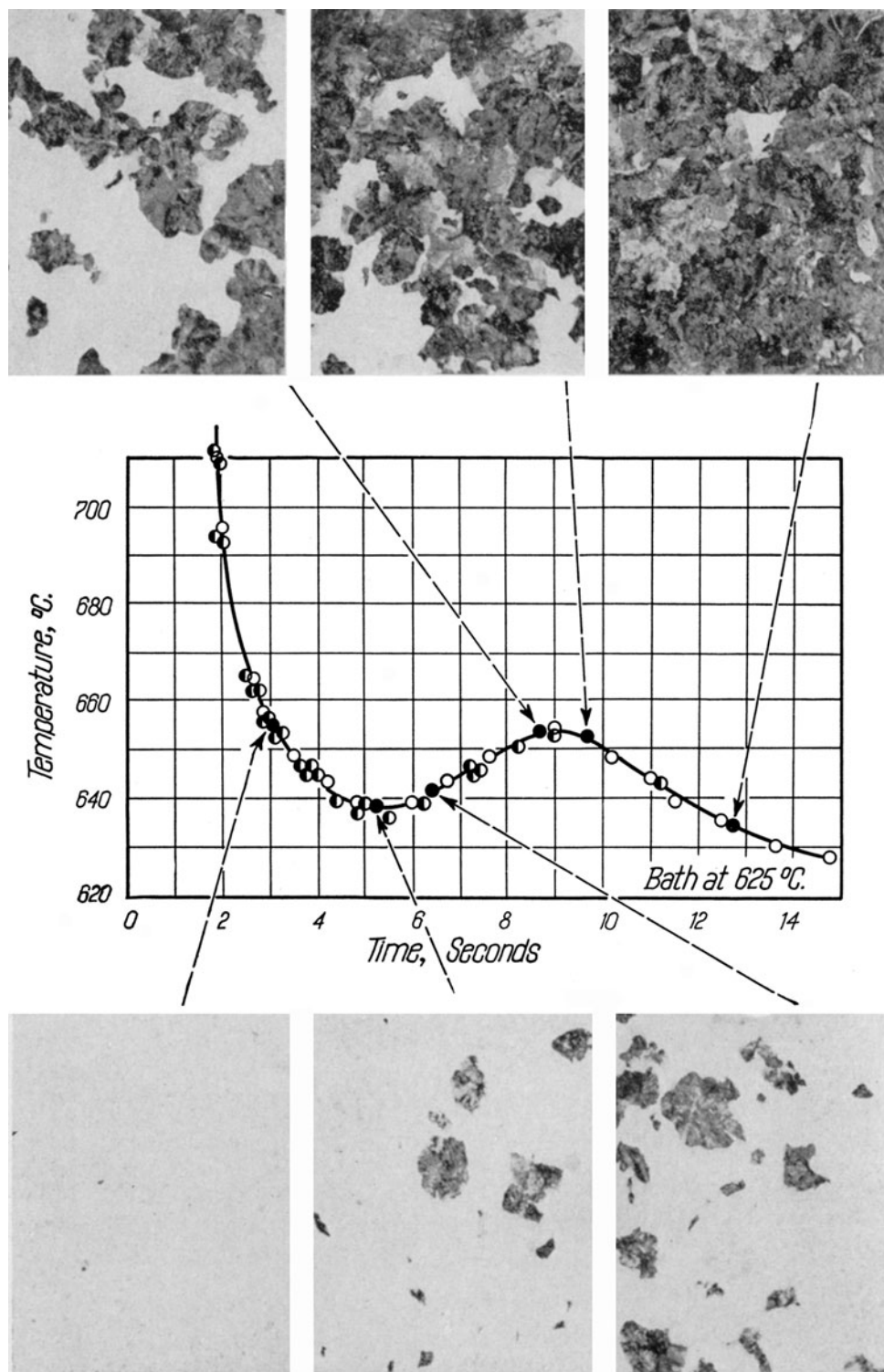


Fig. 4 Correlation of the progress of the reaction with cooling curves for quenching into lead at 625 °C, by quenching into brine at various stages



described in the earlier paper. The tension tests were made at slow speed on 0.25-inch diameter specimens with a 1-inch gage length; the test results should be the same as would be obtained with a standard 0.505-inch specimen with a gage length of 2 inches. It will be observed for Steels A, B, and C that the mechanical properties of bainite

and pearlite are distinctly different, and that there is a transition range of temperature (in which both pearlite and bainite may be detected in the specimens) for which the properties are intermediate between those to be expected of samples entirely pearlite or entirely bainitic. For Steel D, the 3.5% manganese steel, only the properties in the

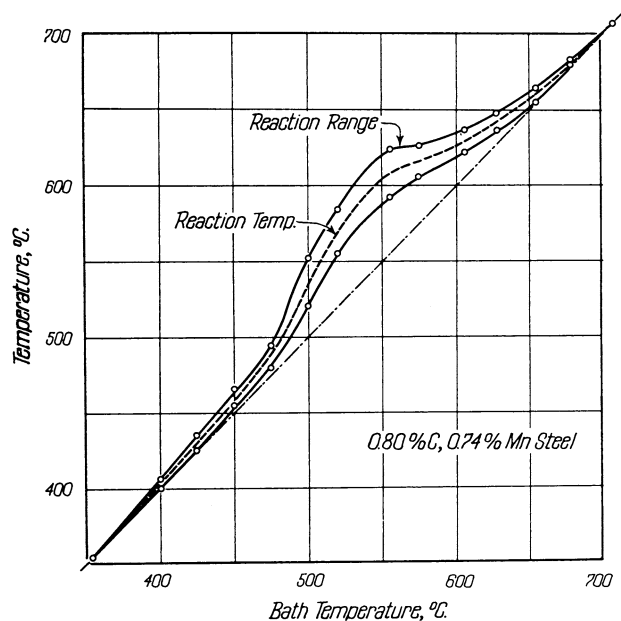


Fig. 5 Reaction temperature versus bath temperature, plain carbon eutectoid steel cylinders, 0.26-inch diameter. Solid lines upper and lower limits of the reaction range, dashed line mean reaction temperature

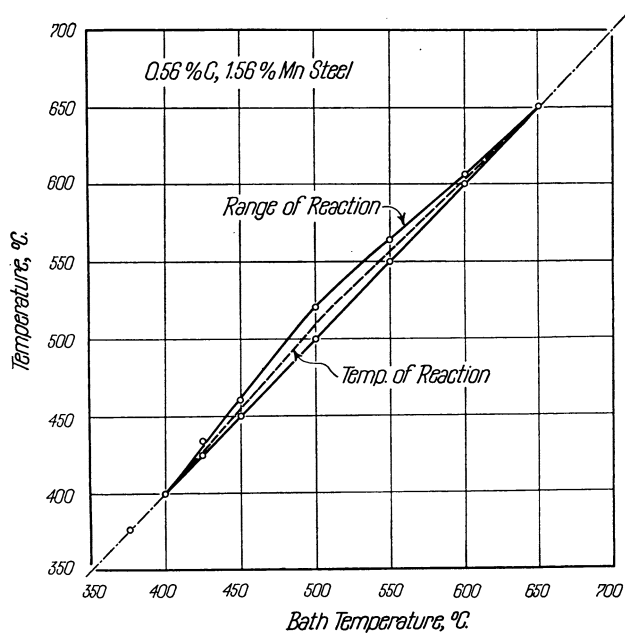


Fig. 6 Reaction temperature versus bath temperature, 0.56 carbon–1.56 manganese rail steel cylinders, 0.26-inch diameter. Solid lines upper and lower limits of the reaction range, dashed line mean reaction temperature

pearlite range have been reported; efforts to react this steel completely at lower temperatures were unsuccessful, for apparently some austenite remains after even very long times at temperatures below those indicated in Fig. 10.

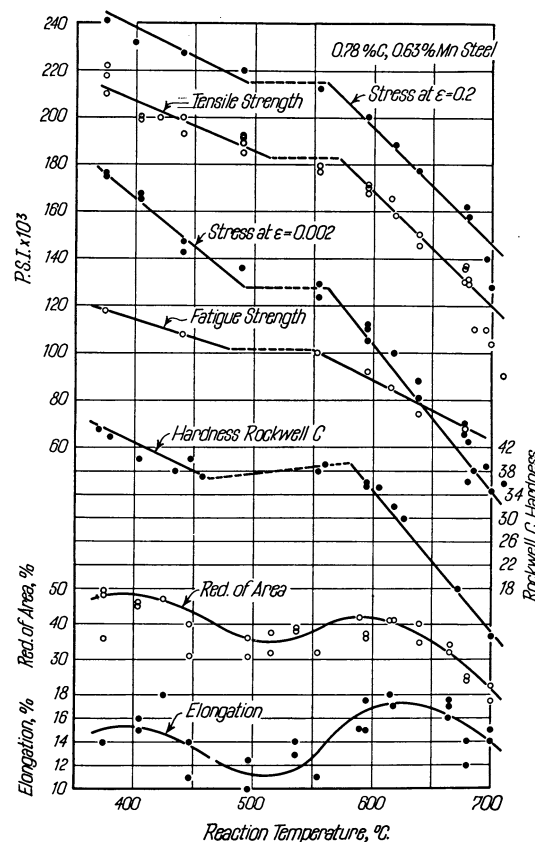


Fig. 7 Mechanical properties versus mean reaction temperature, plain carbon eutectoid Steel A. All specimens furnace-cooled after reaction

Attention should be called to the regularity with which the points for tensile strength, yield strength, and Rockwell hardness fall upon straight lines against the reaction temperature in both the bainite and pearlite ranges.

The variation of ductility with reaction temperature (Figs. 7–10) is of special interest. There seems to be an optimum reaction temperature for best ductility in both the bainite and pearlite ranges. The lack of ductility at the lowest temperatures may be associated with the formation of some martensite, although the reaction times and temperatures make this seem unlikely. The coarse pearlites also are characteristically deficient in ductility. The specimens in the mixed structure range may lack ductility because the structure is mixed, or because either coarse bainite or fine pearlite is brittle. No explanation for this variation of ductility is advanced.

Typical tensile stress strain curves for these steels are plotted in Fig. 11. These curves are so-called “true stress strain curves” in which are plotted the load divided by the corresponding least area of the specimen, against the effective deformation ($\epsilon = \log_e \frac{A_0}{A} = 4.606 \log_{10} \frac{d_0}{d}$) through the point of necking-down and all the way to

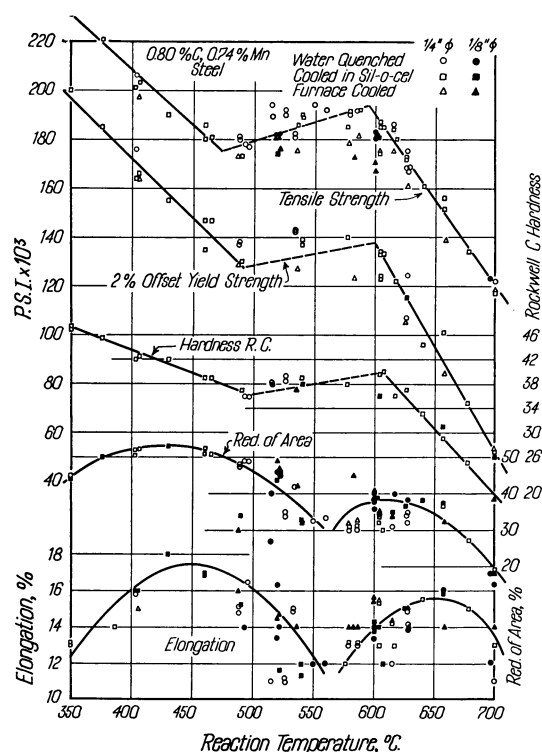


Fig. 8 Mechanical properties versus mean reaction temperature, plain carbon eutectoid Steel B. Open points $\frac{1}{4}$ -inch specimens; filled in points $\frac{1}{8}$ -inch specimens, in sil-o-cel; and triangles furnace-cooled

fracture. Note the yield point in the spheroidized specimens, and its absence in the others.

The static crack strength of all four steels has been plotted in Fig. 12. The method and significance of static crack strength measurements have been discussed in a recent paper by one of the authors [2]. The results reported here are for shallow cracks at the base of $\frac{3}{64}$ -inch deep notches in $\frac{1}{4}$ -inch diameter tensile test specimens. All the test results have been thrown together on one graph to show how nearly alike are the results for all the steels. Figure 12 seems to indicate that the static crack strength, like the other strength indices is different for the bainites and pearlites; that is, the points of Fig. 12 group about two lines, one for the range 355–475 °C (670–887 °F) and another for the range 600–700 °C (1110–1290 °F), with intermediate results for the intermediate temperature range; but the scatter of the test results in the measurement of this property is too great to permit such an observation to be made with confidence. The thing of importance shown by Fig. 12 is that those specimens in the intermediate temperature range of mixed structures which show little ductility in the tensile test, are not deficient in strength in the presence of a crack sufficiently sharp and deep to prevent any but the most localized deformation before fracture. The same is true for those low reaction temperature structures

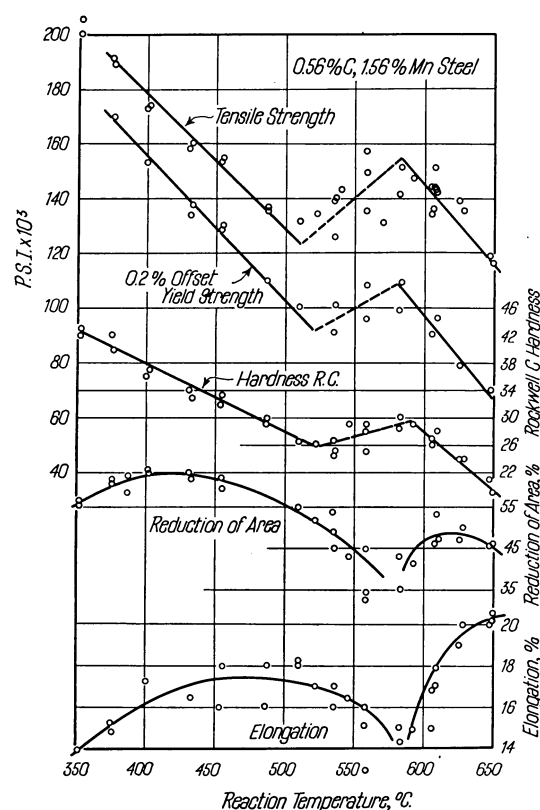


Fig. 9 Mechanical properties versus mean reaction temperature, high manganese rail Steel C. All specimens quenched in water after reaction

which for Steels B and C are deficient in tensile ductility. This illustrates the futility of trying to use ordinary tension tests to estimate the value of a steel for an application requiring strength in the presence of severe stress raisers.

Structure Analysis

The primary purpose of the paper, as stated in the introduction, is the quantitative correlation of properties with microstructure; for this purpose it is necessary to measure the dimensions of the aggregates studied. For the spheroidized samples, the mean uninterrupted straight path through the ferrite has been measured and for the pearlites the mean interlamellar distance. From the latter has been calculated the mean uninterrupted straight path through the ferrite; and this value used as a basis for comparison of the pearlite and spheroidite of Steel B.

The pearlite spacing was determined by measuring the fraction of the area of a polished and etched surface that could not be resolved with a microscope objective of known resolving power, or the fraction with an apparent or surface spacing less than some selected value; followed by the application of a formula derived by a simple integration

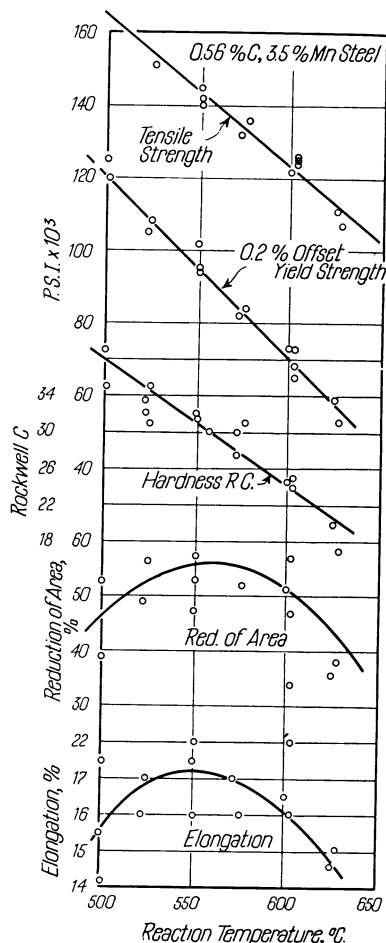


Fig. 10 Mechanical properties versus mean reaction temperature, 3.5% manganese eutectoid Steel D. All specimens cooled in sil-o-cel after reaction

on the assumption of entirely random orientation of the pearlite plates with respect to the plane of polish. The formula is $S_0^2 = S^2(1 - N^2)$ where S_0 is the mean true spacing, and N is the fraction of the surface with an apparent spacing less than S [3].

The procedure was to trace the boundaries of the unresolved areas on thin paper stretched on the plane glass of the microscope camera, then to measure the areas either by cutting up the paper and weighing the pieces, or with a planimeter. No great accuracy was achieved, but fortunately none is necessary, for the relationship between the reaction temperature and the spacing, as well as the tensile properties and the spacing, is a semilogarithmic one, with the logarithm of the spacing plotting as a straight line against the properties and the temperature; considerable change in spacing is associated with a change in reaction temperature or properties corresponding to the experimental error and reproducibility of the measurement of these quantities. The extent to which the error of

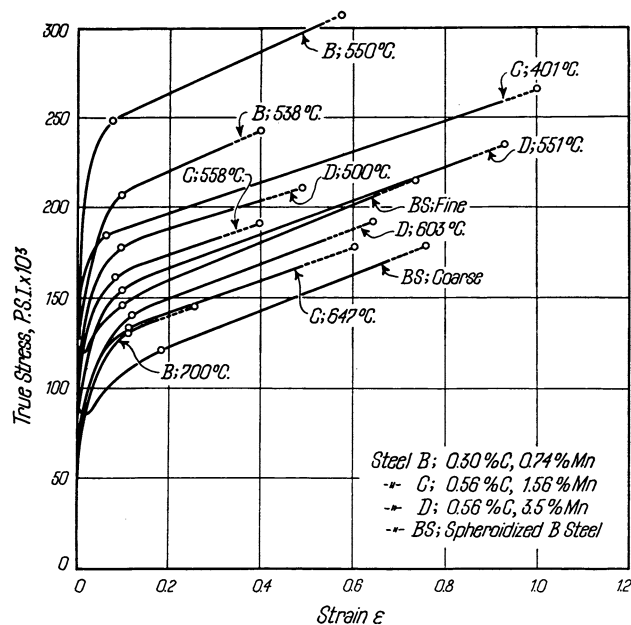


Fig. 11 Typical stress-strain curves. “True stress” ($\sigma = \frac{P}{A}$; load divided by the corresponding least area) versus effective deformation ($\epsilon = 4.606 \log \frac{d_0}{d}$)

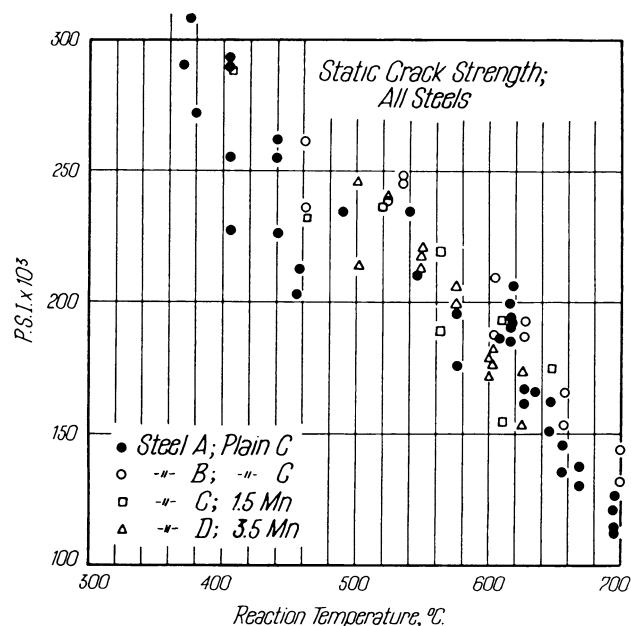


Fig. 12 Static crack strength versus mean reaction temperature, all steels. Solid circles Steel A, plain carbon; open circles Steel B, plain carbon; squares Steel C, 1.5 manganese; triangles Steel D, 3.5 manganese

measurement affects the results may be estimated from the scatter of the points in Figs. 13 and 15.

The pearlite spacing measurements are plotted in Fig. 13, in the upper plot against the reaction temperature and in the lower plot against the reciprocal of the reaction

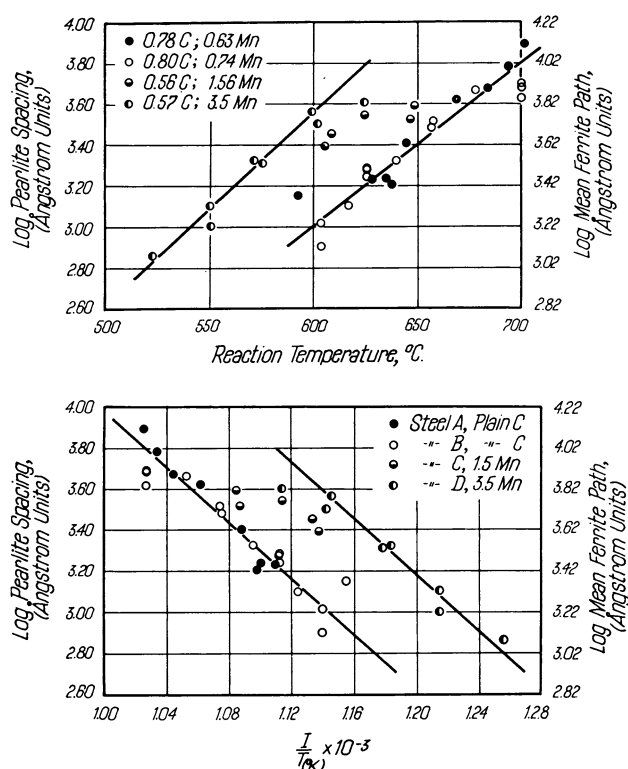


Fig. 13 Pearlite spacing (distance from center to center of the cementite plates in Angstrom units) and mean uninterrupted ferrite path in pearlite versus the mean reaction temperature, *top*, and the reciprocal of the absolute temperature, *bottom*

temperature on the absolute temperature scale. A straight line on the reciprocal temperature plot transfers to the direct temperature plot as a curved line, but so slightly curved that it can hardly be distinguished from a straight line over the temperature range covered by the measurements. Theory suggests [4] the reciprocal temperature plot; obviously these measurements do not provide a test of the theory. The lines of Fig. 13 are drawn to have the same slope as the line drawn by Wells and Mehl [5] through their data for the logarithm of the time rate of diffusion of carbon through austenite and the diffusion temperature. A line of this slope fits the data for the pearlite spacing as well as any that could be drawn.

In the spheroidized steel the average distance between spheroids along straight lines drawn across photomicrographs at $\times 4000$ was measured, using about 250 measurements for each specimen. The particles are of course only approximately spheroids and occur in a range of sizes, the small ones more numerous than the large ones.

The mean uninterrupted straight path through the ferrite in a coarse pearlite was measured in the same way as for the spheroidized specimens. A great many photomicrographs from one specimen with uniform and coarse, well developed pearlite, were available from a study current in

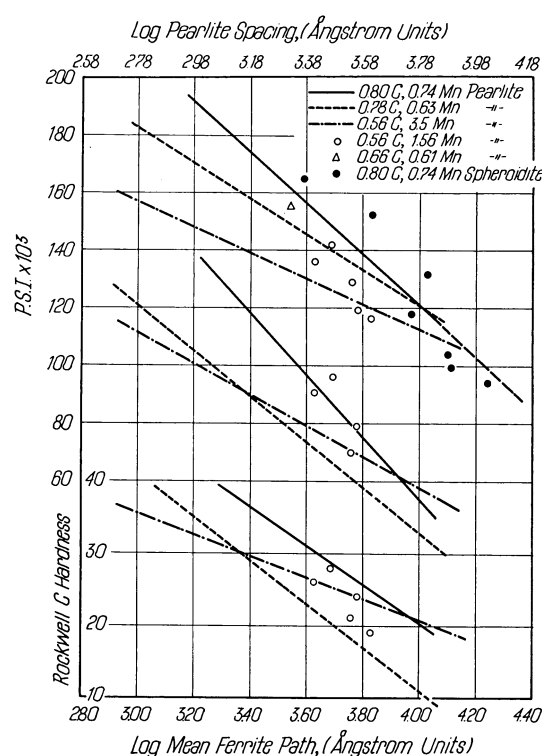


Fig. 14 Mechanical properties versus mean uninterrupted ferrite path for all pearlitic steels and spheroidized Steel B (0.80 carbon, 0.74 manganese). Individual points for the pearlitic steels are shown only for the 1.5 manganese Steel C and one point for the pearlite hypoeutectoid 0.66 carbon, 0.61 manganese steel. *Top* group tensile strength, *middle* group yield strength (0.2% offset), *bottom* group Rockwell hardness

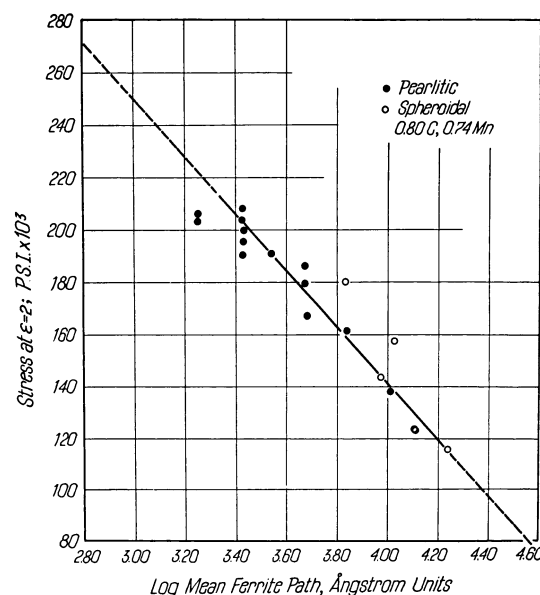


Fig. 15 Stress at $\epsilon = 0.20$ versus mean ferrite path for Steel B, in both the pearlitic and spheroidal conditions

the laboratory, and these were used. The mean interlamellar spacing was determined as described above. It was found that the mean uninterrupted ferrite path is between 1.9 and 2.0 times the interlamellar spacing. This corresponds to the theoretical mean path between plates for ideal, plane plates up to an angle from the perpendicular of 77.5° , or to within 12.5° of parallelism with the plates. Considering the size of the pearlite colonies and the waviness of the plates, this seems a reasonable figure, and it has been used to calculate the mean ferrite path from the interlamellar spacing for all the pearlites measured. In Fig. 13 the ferrite paths so calculated are indicated.

Properties Versus Structure

Figure 14 summarizes the test results on those samples for which the dimensions of the aggregate have been measured. For the pearlites, the lines have been drawn by transferring the straight lines from the plots of properties against reaction temperature (Figs. 7–10) and the plot of spacing against reaction temperature (Fig. 13), thus deriving the straight lines of Fig. 14 for properties against spacing. On the upper edge of the figure is indicated the scale for the interlamellar spacing of the pearlites by which is meant the mean *least* distance between the plates. Along the bottom edge of the plot is indicated the mean uninterrupted path through the ferrite for both the pearlites and spheroidites; this mean path has been experimentally determined as previously described. The extent to which the mean path in the ferrite controls the properties of these measurable aggregates is obvious from the graph.

In Fig. 15, the true stress corresponding to an effective deformation (ϵ) of 0.20 is plotted against the mean straight path through the ferrite for both pearlitic and spheroidal specimens of Steel B. This strength index is not affected by variations in the yield point behavior, whether caused by structure or previous mechanical treatment, and corresponds to a given amount of cold work better than does the tensile strength. (It may be seen from Fig. 11, in which the stress and strain corresponding to the maximum load or tensile strength is indicated on each curve by a filled-in circle that the strain at the maximum load varies considerably.) It will be observed in Fig. 15 that the points for the spheroidized steel fit the line almost as well as the points for the pearlitic steel; this is not brought out in Fig. 14, in which the individual points for the pearlitic specimens are not shown.

In Figs. 14 and 15, the mean ferrite path through the pearlite has been taken to be 1.9 times the interlamellar spacing. If the ratio 2.0 had been used, the points for the spheroidized steel would have been displaced to the right with respect to the line for the pearlite by 0.02 on the

logarithmic spacing scale; this is the limit by which the results are likely to be in error, and it is not enough to affect the conclusions drawn from the data.

There is an interesting influence of the microstructure on the yield point (not to be confused with the yield strength by the off-set method). In the pearlites and bainites, no yield points were observed even in the samples containing the coarsest pearlite. The spheroidites, on the other hand, all are characterized by well-developed yield points, both upper and lower, with a yield point elongation is in annealed low carbon steel. A slight yield point was observed in coarse pearlite held too long at the reaction temperature; it probably is caused by partial spheroidization.

The lower yield point of the spheroidized steel is from 80 to 90% of the tensile strength, with the smaller figure applying to the coarsest structures and the larger to the finest. As a result of this yield point the 0.2% off-set yield strength for the spheroidized specimens lies well above the yield strength for the pearlitic specimens of the same tensile strength. The ratio of the 0.2% off-set yield strength to the tensile strength for the coarse pearlite in the same steel (B) is only 44%, which rises to 73% for the finest pearlite; for the bainite it is 78% at the high end of the reaction temperature range and 84% at the lowest temperature studied.

It has not been thought necessary to illustrate the microstructure for each specimen; photomicrographs of typical structures, excepting the simple pearlites, are collected in Figs. 16–18.

Discussion

It has been known for a long time that finer aggregates are stronger than coarser. In pearlitic steels, the coarser the pearlite the softer the steel. In the spheroidal or nonlamellar structures, the same is true; coarse spheroidite, or spheroidized pearlite, is much softer than the barely resolvable structures resulting from the tempering of martensite, generally known as sorbite. Fine eutectics in other alloys are harder and stronger than coarse. But the relationship between strength on the one hand, and the dimensions of the particles or interparticle distances on the other hand, has remained wholly qualitative. The ductility of aggregates is not even subject to such a qualitative generalization; there is no well recognized connection between the capacity for deformation of metals and the size or spacing of the particles in the structure. It seems clear that if the factors that control the properties of alloys are ever to be really understood, a quantitative rather than qualitative connection between structure and properties must be established.

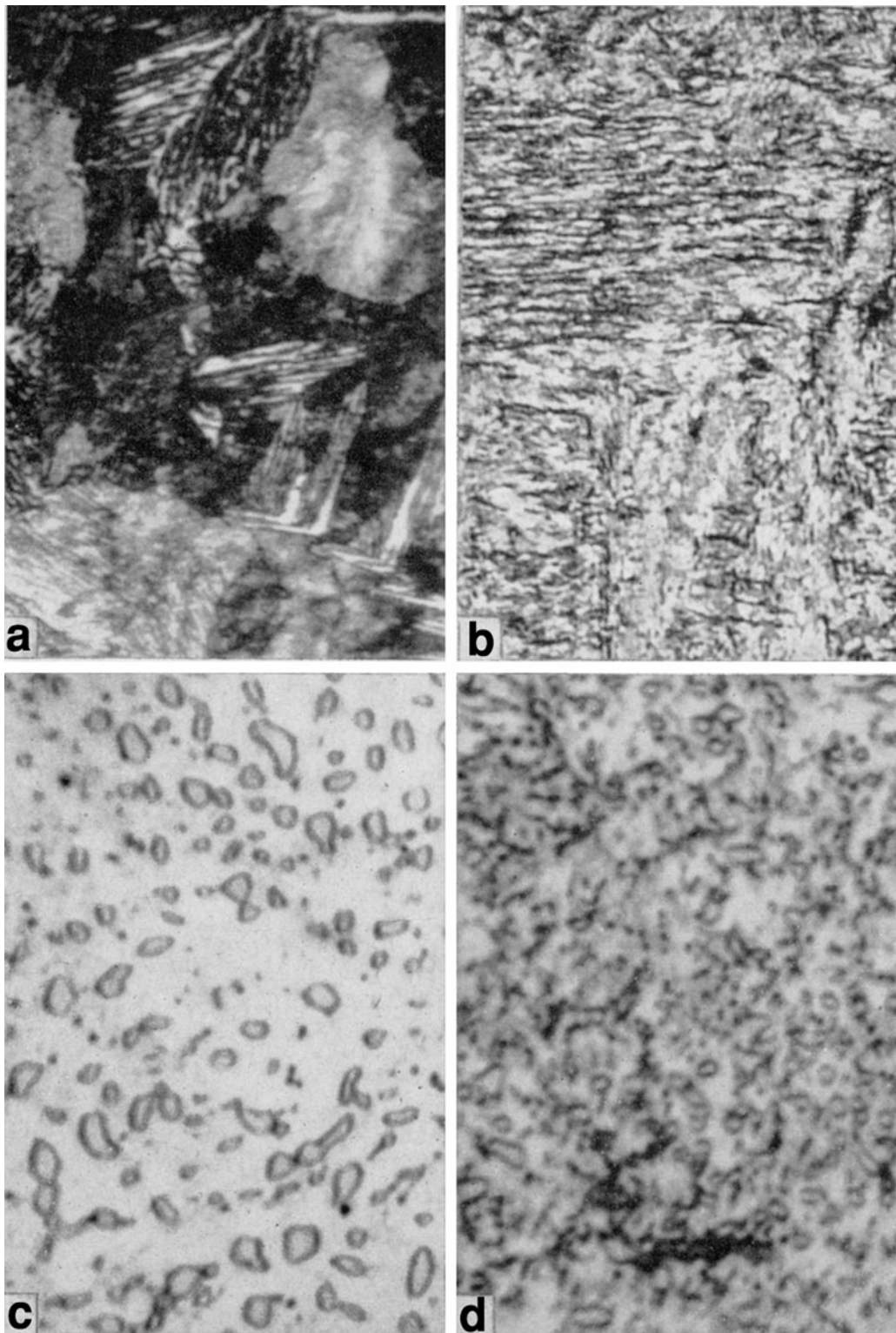


Fig. 16 Steel B, 0.80 carbon, 0.74 manganese. **a** Reacted 2 min at 553 °C \times 2000; picral + nital. **b** Reacted 20 min 406 °C \times 2000; ferric chloride. **c** Quenched in oil from 750 °C, tempered 2 h

695 °C \times 4000; nital. **d** Quenched in oil from 750 °C, tempered 12 h 498 °C \times 4000; Nital

It might be thought that such information could be obtained by a careful correlation between mechanical test results and microstructure, using the almost innumerable

papers that have been appearing for many years containing both test results and photomicrographs of the specimens, or similar data in the files of many steel producers and

consumers. The difficulty with this procedure is that almost never are the specimens uniform enough in structure to make it possible. Unless special precautions are taken to insure uniformity, which in steel means control of the austenite decomposition temperature among other factors, the correlation is uncertain because of the unknown effects of mixed microstructures. Again, all possible variations in structure should be studied in one alloy, to eliminate the variations caused by differences in composition and properties of the individual phases within the aggregate structures. In the present paper, these precautions have been taken.

In this paper the development of a theory of the strength of alloys has been advanced by the demonstration of what might be a natural law of strength for aggregate structures, which may be stated as follows: *The resistance to deformation of a metallic aggregate consisting of a hard phase dispersed in a softer one is proportional to the logarithm of the mean straight path through the continuous phase.*

By the mean straight path is meant the average distance in all directions from one hard particle to another; in lamellar structures this means the average distance from one plate to the adjacent one, not in the direction perpendicular to the plates which is the shortest distance, but averaged for all directions from perpendicular to parallel to the plates. If the pearlite colonies were infinite in size and the plates were perfectly plane, this average would be infinite; but the plates are always wavy and the pearlite colony size is always limited, so it turns out by measurement that the average distance is between 1.9 and 2.0 times the least distance separating the plates.

The numerical value of the ratio between the pearlite spacing and the mean ferrite path will be affected by any variation of the effective waviness of the plates and hence may vary with the reaction temperature and such factors as austenite grain size and relative rates of nucleation and growth of the pearlite colonies. The value may also need modification to take into account the fact that the cementite plates delineate definite crystallographic planes in the ferrite and that slip occurs on definite planes, so that the mean path, considering all directions, may not actually be the mean path considering these crystallographic limitations. The experimental scatter in test results and spacing measurements makes it unlikely that these refinements will be possible.

It is true that the validity of the law has been demonstrated only for the structures obtained in steel, and even there with perhaps too few tests and too few steels, although the work reported here has taken the full time of two people in the laboratory for about 3 years. It is hoped that the work will continue and extend to more steels, more treatments, and to nonferrous alloys. It is also hoped eventually to explain the variations of ductility with structure that have been observed in this study.

It is possible to explain the semilogarithmic relationship between strength and mean path through the softer phase, as described above, in a simple way. In the explanation offered below, the word “dislocation” is used, as introduced by Taylor [6] to describe what might also be called a single, elementary slip; whether we accept Taylor’s concept of the nature of the elementary slipping process, or unit slip, is not important in this explanation, although the dislocation is such a reasonable picture of the nature of the fundamental gliding process that it seems best to use it until another mechanism of slipping is suggested.

It is generally held that a dislocation traverses, not an entire crystal, if the crystal be large, but only a part of the crystal. Crystals are supposed to be divided, by imperfections of one sort or another, into “blocks”; the boundaries between these crystal blocks are considered, after Taylor, to be “semi opaque” to the propagation of dislocations. By this it is meant that at some points along the boundary between two blocks, dislocations can cross the boundary, but at others, dislocations cannot move from one block into the other because the lattices of the two blocks do not match well enough at the latter points. Let us designate by the letter L the average distance in a large crystal through which a dislocation, or unit slip, may travel.

If particles of a hard phase are introduced into the crystal, these will serve as completely opaque boundaries, blocking the passage of dislocations, and limiting the distance that can be traversed by a dislocation to the average distance from particle to particle through the matrix. Call this average dislocation path x ; it is the mean straight path through the soft phase referred to above. Now if N dislocations are needed to produce a certain macroscopic strain in a single crystal in which the mean dislocation path is L , then, if hard particles are so distributed throughout this same crystal as to reduce the mean dislocation path to x_1 , the number of dislocations needed to produce this same strain will be $\frac{L}{x_1} \cdot N$; and if the particles are so distributed as to reduce the mean path to x_2 the number needed will be $\frac{L}{x_2} \cdot N$. Hence the ratio of the number of dislocations needed in two aggregates with paths x_1 and x_2 will be $\frac{LN}{x_1} / \frac{LN}{x_2}$ or $\frac{x_2}{x_1}$; and to produce strain at a certain rate, dislocations will need to be generated at rates which are to each other as x_2 is to x_1 ; that is, $\dot{N}_1 / \dot{N}_2 = x_2 / x_1$; where \dot{N}_1 and \dot{N}_2 are the time rates at which dislocations must be generated to produce flow at a certain rate of straining in specimens with mean dislocation paths x_1 and x_2 , respectively. If we knew the relation between the rate of formation of dislocations and the applied stress, we would know the effect of the mean dislocation path on the resistance to deformation at constant strain and constant strain rate. The relation between speed of deformation and stress is thought to be

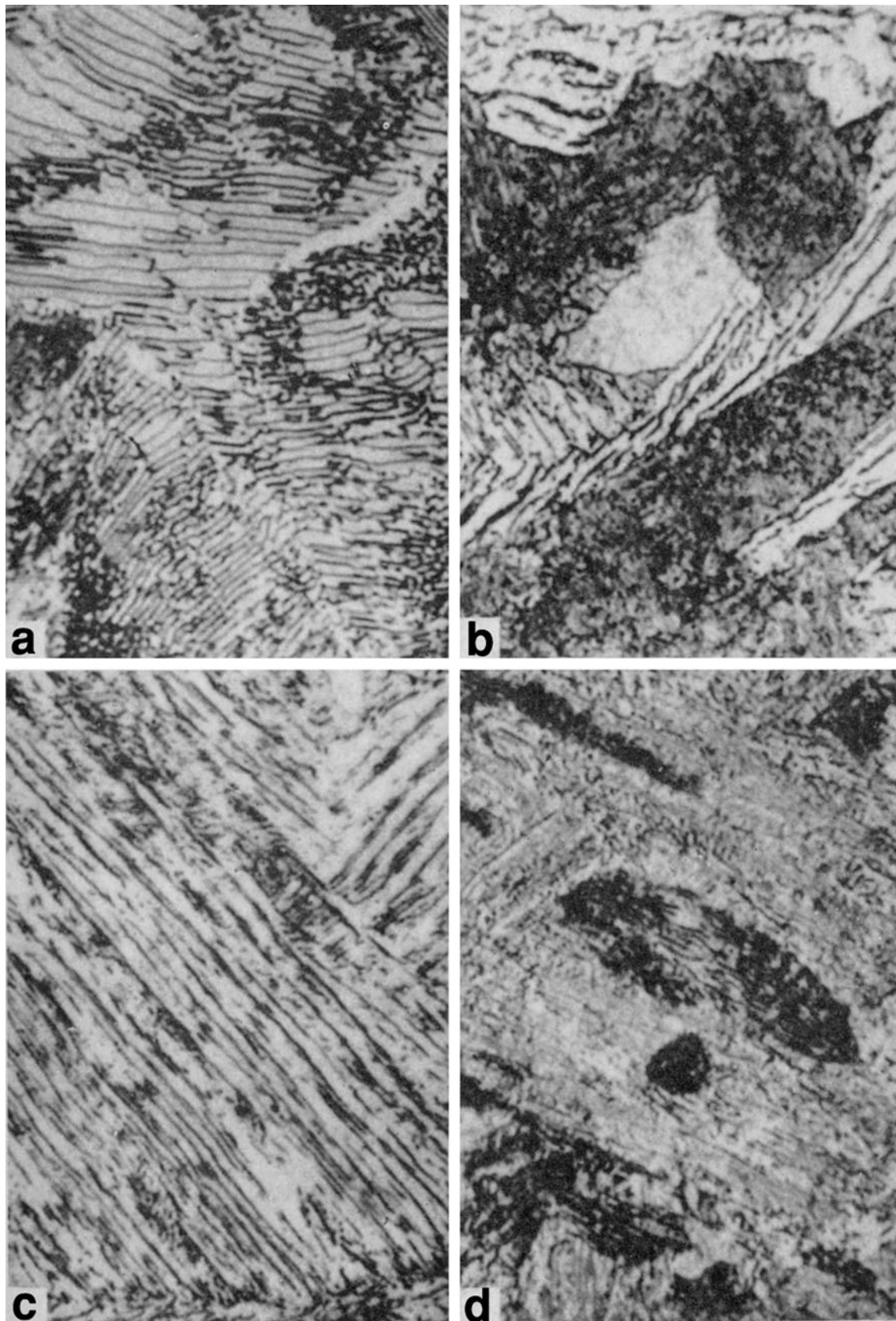


Fig. 17 Steel C, 0.56 carbon, 1.56 manganese. **a** Reacted 30 min 646 °C \times 2000; nital. **b** Reacted 3 min 558 °C \times 2000; nital. **c** Reacted 3 min 510 °C \times 2000; nital. **d** reacted 4 min 456 °C \times 2000; picral + HCl

semilogarithmic; the logarithm of the rate of flow plots as a straight line against the stress, at least for steel and copper at relatively low temperatures [7–10].¹ If we take the speed of deformation to be proportional to the rate of generation of dislocations, \dot{N} , then $\log(\dot{N}_1/\dot{N}_2) = a(\sigma_1 - \sigma_2)$ where σ is the stress and a is a constant. From the proportion above, $\dot{N}_1/\dot{N}_2 = x_2/x_1$, write $\log(x_2/x_1) = a(\sigma_1 - \sigma_2)$, which plots as a straight line for the logarithm of the spacing against the stress, as in Fig. 14. It is realized that this theory is far from complete and no doubt greatly oversimplified.

It was thought advisable to test the range of application of the proposed law by making an effort to calculate the size of the particles in the tempered steel of the highest strength attainable upon complete elimination of martensite, using the data obtained from much coarser structures. To do this requires a method for the calculation of the mean ferrite path as a function of the size and amount of carbide particles. This is obtained as follows: Take the particles to be spheres of radius r . Imagine a bundle of dislocations leaving one such sphere and traveling in parallel directions at the same speed, v . In time t the volume of material traversed will be $\pi r^2 vt$. If there are n spheres per unit volume of alloy, then the number of spheres in the volume traversed will be $\pi r^2 vtn$. The length of the cylindrical volume traversed is vt . Then the average distance from particle to particle will be this length divided by the number of spheres in the volume $vt/\pi r^2 vtn$, or $x = 1/\pi r^2 n$ where x is the mean ferrite path. The number of spheres per unit volume, n , is easily calculated from the volume percentage of the phase, which in turn is calculated from the weight percent of carbon and the densities of ferrite and cementite. When this calculation is carried out for an 0.80 carbon steel on the assumption that 300,000 pounds per square inch is the maximum tensile strength that can be developed (no martensite present) and using the data summarized in Fig. 14 to estimate the ferrite path x for this tensile strength, the diameter of the carbide particles, assuming them to be spheres, calculates to be about 17 Å. Since the orthorhombic unit cell of cementite has the dimensions $4.5 \times 5.1 \times 6.7$ Å it is thought that this result indicates fair agreement between experiment and theory, and lends support to the wide application of the law of strength advanced in this paper. An average diameter of 6.7 Å (equal in volume to one unit cell) would be too small to be expected, and requires a tensile strength of 338,000 pounds per square inch, which is certainly higher than

would be expected in completely tempered steel. An average diameter of 20 Å (about 3 unit cells) should have a tensile strength of 295,000 pounds per square inch and is probably nearer the value than can be realized experimentally. In Table 2 is listed the tensile strength calculated for spheres of various diameters in multiples of the unit cell of cementite. One thing brought out by such a table is the large effect on the strength produced by particles of small size, and the relatively minor effect associated with a change in size when the particles are larger, although still quite small. This helps to explain the marked strengthening brought about by small amounts of impurities or alloying elements when finely dispersed, as in age hardening systems.

It is interesting to calculate the average dislocation path to be expected in this steel after complete decarburization, or after spheroidization to very large carbide particles. Assuming that a tensile strength of 60,000 pounds per square inch could be reached, the mean ferrite path calculates to be 50,000 Å, which is 5 μm (5 mm at 1000 diameters magnification). This is of the order of magnitude to be expected for several imperfection blocks, and is then in line with our expectations concerning the limiting strength of polycrystalline aggregates of this ferrite. Grain size should not affect the tensile strength until the grains become smaller than this size; experiments carried out by two of the authors but not yet ready for publication indicate that, for grain sizes considerably >5 μm, it is true that grain size does not affect the tensile strength if the size of the tensile test specimen is always so chosen as to contain the same number of grains.

One experiment was performed to test whether or not the *amount* of the hard, dispersed phase is a variable affecting the resistance to deformation. It was observed, as may be seen in Fig. 14, that the strength of the 1.5 and 3.5% manganese steels is if anything lower than the strength of the plain carbon steel, rather than higher as might be expected for the same spacing if the ferrite were strengthened by the solution of manganese. These steels are lower in carbon, and it was suspected that the lesser amount of carbide in the structure might be responsible for this, in spite of approximately the same spacing. The ferrite in these steels should be no weaker, unless the relatively large amount of silicon, copper and nickel in Steel B is responsible for its greater strength, which may well be; manganese is not thought to be very effective in strengthening the ferrite in steel. It was thought advisable to determine the strength of hypoeutectoid steel of about the same chemical analysis in the ferrite as the eutectoid Steel B. A bundle of wire rod with 0.66 carbon and 0.61 manganese was obtained from the manufacturer of Steel B (for which the data on spheroidized structures were also obtained) and reacted by quenching into lead at 631 °C

¹ The semilogarithmic law is also suggested by Kauzmann's application of the Eyring general theory of shear rates, although the authors are inclined to the opinion that his remarks apply to the generation of dislocations rather than their movement.

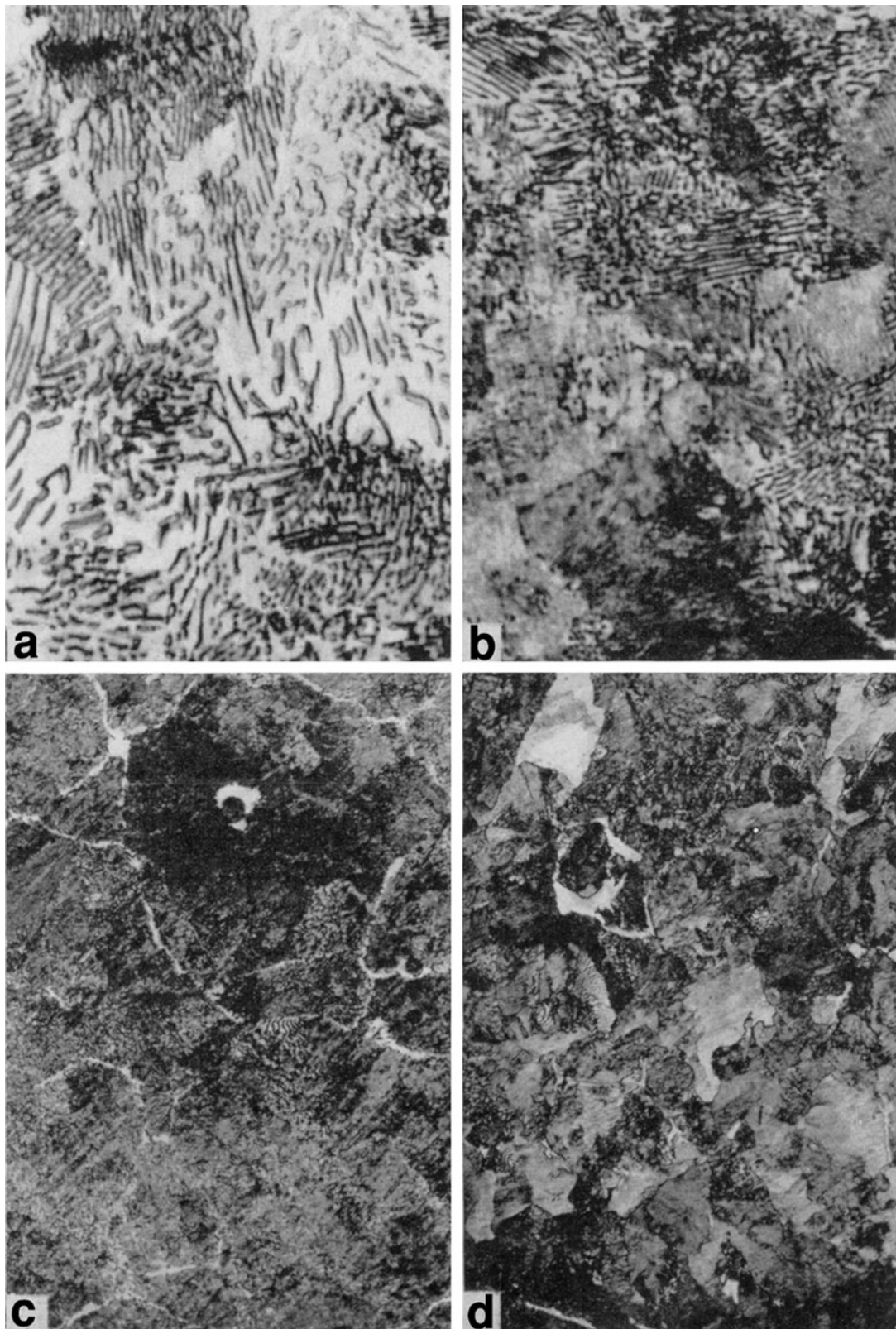


Fig. 18 **a** Steel D (0.57 carbon, 3.5 manganese) reacted 2 h 628 °C × 2000; nital. **b** Steel D (0.57 carbon, 3.5 manganese) reacted 4 h 603 °C × 2000; nital. **c** Steel C (0.56 carbon, 1.56

manganese) reacted 30 min 646 °C × 300; nital, showing excess ferrite. **d** Steel E (0.66 carbon, 0.61 manganese) treated 15 s 631 °C × 300; nital, showing excess ferrite

Table 2 Calculated tensile strength of 0.80 carbon steel

Average spheroid diameter in unit cells (6.66 Å)	Tensile strength pounds per square inch
1	338,000
2	311,000
3	295,000
4	284,000
5	276,000
6	268,000
7	262,000
8	257,000
9	253,000
10	249,000

(1165 °F) to produce a structure which was almost free from proeutectoid ferrite, although some was present (see Fig. 18d). The tensile strength of two specimens so treated is almost identical with the tensile strength of the eutectoid steel of the same pearlite spacing (the tensile strength of both hypoeutectoid specimens is indicated by the triangle in Fig. 14). This result, together with the suspicion that the structure of the higher manganese steels is not entirely pearlitic, or at least is pearlite so distorted as to make the spacing measurements untrustworthy, leads to the conclusion that the amount of the hard, dispersed phase, within limits that have not yet been determined, exercises no control over the strength of the aggregate structures. Further tests on this subject are in progress.

There is some evidence that the strength of mixed structures obeys a simple rule of mixture, without anomalous strength or weakness. Examination of Figs. 8 and 9 reveals that the strengths of the specimens in the temperature range for mixed structures are intermediate between the values expected by extrapolation of the straight lines for the unmixed pearlite and bainite structures. This may be explained by supposing the amount of each structure present to be a function of the reaction temperature within the mixed structure range, and the spacing and properties of the pearlite and the bainite in the mixed structure to be obtainable by extrapolation from the temperature range in which each is found alone. If this is so, then it would seem that no anomalous property changes are to be expected in specimens of nonuniform microstructure, but rather that the strength would be known if the amounts and properties of each structure in the aggregate were known. Obviously no such conclusion can be drawn about tensile ductility, for which there is a sharp minimum for mixed structures in Figs. 8 and 9.

It may be well to emphasize the difficulty of obtaining uniform structures in steel. The recalescence studies for

lead quenched specimens big enough for tensile tests show that when the lead bath temperature is near the temperature of fastest reaction, the reaction product is formed over a considerable range of temperature. Perhaps the heterogeneity of structure resulting from this cause is responsible for the deficiency of ductility in the mixed structure range. Steel A shows more ductility in this range than Steel B, and also shows a shorter temperature range over which mixed structures are obtained. As mentioned before, it does not yet seem possible to put forth a theory explaining the variations in ductility observed.

The similarity among the stress–strain curves for all the steels is worth comment (Fig. 11). The slope of the stress–strain curve in the plastic range varies only slightly with composition and treatment. The yield point behavior of the spheroidized specimens has been remarked upon; no explanation is advanced. It may be seen that softer pearlitic specimens show no such yield point. It may be, as has been frequently suggested, that the yield point in iron is a grain boundary effect (single crystals of iron do not exhibit a yield point) and that in spheroidized samples the ferrite boundaries have an opportunity to exercise an effect that is impossible in pearlite. The greater ductility of the spheroidites may also be observed.

These experiments provide information of interest concerning the nature of bainite. Mehl [4] and others have suggested that bainite forms by a different mechanism than pearlite and that it may be structurally quite different. The width of what appear to be ferrite bands in high temperature bainite is greater than the interlamellar spacing of fine pearlite formed at a higher temperature. Bainite assumes an acicular habit whereas pearlite prefers to grow into nodules. Smith [11] has found that the orientation relationships between austenite and bainite and between austenite and martensite are similar, and both are different from the austenite and ferrite-in-pearlite relationship [12], which indicates a different process of nucleation, as suggested by Mehl. The observations reported above concerning the strength of bainite and pearlite may be interpreted to mean that pearlite and bainite are quite different products, in line with previous suggestions and particularly in accord with the orientation relationship studies of Smith. The lower strength of bainite at its highest formation temperature indicates that it is a coarser structure than pearlite at its lowest formation temperature; in the range of mixed structures the bainite may be the coarser of the two structures present.

In conclusion it is desired to comment on the excellence of agreement between the slopes of the plot of the logarithm of the diffusion coefficient for carbon in austenite against the reciprocal of the absolute temperature, as determined by Wells and Mehl [5], and the slope of the plot of the logarithm of the pearlite spacing against the

reciprocal of the absolute temperature of the reaction, shown in Fig. 13, in which all the lines are drawn with the same slope as the line drawn by Wells and Mehl through their points. This provides the first direct evidence of what has long been assumed, that the spacing of pearlite is controlled by the rate of diffusion of carbon in austenite. It further shows that the spacing is directly proportional to the carbon diffusion rate.

Wells and Mehl have shown that the slope of their log D versus $1/T$ plot (this slope is Q/R where Q is the activation energy and R the gas constant) is not affected by carbon content. They have also shown that at 1000 °C (1830 °F), manganese and nickel have little effect on the diffusion coefficient. Since these elements have practically no effect on the diffusion coefficient at 1000 °C (1830 °F), it is fair to assume that they have little effect on the slope of the plot. Hence, it is to be expected that the slope of the plot of the logarithm of the pearlite spacing against the reciprocal of the reaction temperature will be the same for steel of any carbon content and perhaps also for any alloy content; possibly the carbide forming elements are different in this respect. Then a determination of the spacing for a steel reacted at one temperature should suffice to calculate the spacing at any other temperature. To do this, using Fig. 13, draw a line parallel to the lines already there, through the one experimentally determined point, and pick the spacing for any other temperature from the line so drawn.

Summary

1. The factors that determine the mechanical properties of aggregate structures consisting of a soft continuous phase and a hard dispersed one are the specific properties of the continuous phase and the mean uninterrupted path through the continuous phase, whether the structure be lamellar or spheroidal. This has been demonstrated for the aggregate structures pearlite and spheroidite in the same steel.
2. The resistance to deformation (yield strength, tensile strength, hardness) varies linearly with the logarithm of the mean uninterrupted path through the continuous phase.
3. This rule has been shown to be in accord with modern theories of the mechanism of plastic deformation.
4. Calculated tensile strengths for the finest aggregates agree with experimental results in tempered steels, and support the application of the rule over a wide range of particle size.
5. The amount of the hard, dispersed phase is of less consequence than the mean path through the soft, continuous phase.
6. In eutectoid, low alloy steel the tensile strength, yield strength and hardness plot as straight lines against the reaction temperature, but the pearlite line for each lies above the bainite line. Bainite and pearlite probably are not members of the same continuous family of isothermal reaction products as previously suggested.
7. The ductility of the bainites and the pearlites is a maximum in the middle of the temperature range over which each is formed.
8. There is an intermediate range of reaction temperatures in which mixed structures are formed. The tensile strength, yield strength and hardness of these mixed structures lie between the values to be expected of completely pearlitic and completely bainitic steels in this range, but the ductility as measured by both elongation and reduction in area is lower for mixed structures.
9. In isothermal reaction studies of low alloy steels using lead baths for quenching and maintaining the reaction temperature, extreme care must be exercised to be sure that the reaction really takes place at the bath temperature, even with very small specimens; with larger specimens, it is necessary to determine the reaction temperature, which then occurs over a range of temperatures.
10. When recalescence occurs, as it does for all but the smallest specimens when quenched into a bath near the temperature of fastest reaction for low alloy steels, the reaction is about half over at the peak of the temperature time curve, having started not much before the temperature reached its minimum just before recalescence; and the reaction is nearly over by the time the temperature again reaches the same value as this minimum in the cooling curve.
11. Spheroidized eutectoid steel exhibits the kind of yield point familiar in low carbon steel; the same steel in the pearlitic condition and with the same tensile strength has no yield point. The spheroidal structure is markedly superior in ductility to pearlite of the same tensile strength.
12. The static crack strength (tensile strength in the presence of a sharp crack) varies regularly with the reaction temperature in structures formed directly from austenite, and does not reflect the variations of ductility observed in the tensile test.
13. The spacing of pearlite is directly proportional to the coefficient of diffusion for carbon in austenite for any one steel.
14. The known rate of variation of the carbon diffusion coefficient with temperature may be used to calculate the pearlite spacing at various reaction temperatures after it has been determined at one temperature.

Acknowledgments The authors wish to acknowledge the greatly valued support and advice of Dr. Robert F. Mehl, Director, and Dr. Cyril Wells of the Metals Research Laboratory. They wish to acknowledge helpful discussion with Dr. G. V. Smith, Dr. F. C. Hull, Dr. W. A. Johnson, Mr. M. F. Hawkes, and Mr. G. E. Pellissier; the latter prepared the series of photomicrographs of a single specimen of coarse pearlite upon which is based the determination of mean ferrite path in pearlite. Steel A was furnished by the Page Steel and Wire Company, Steel B and the 0.66 carbon, 0.61 manganese steel by the Republic Steel Corporation, Steel C by the Ames-Baldwin-Wyoming Company, and Steel D was made especially for this study by the Research Laboratory of the Union Carbide and Carbon Company, under the direction of Walter Crafts.

References

1. M. Gensamer, E.B. Pearsall, G.V. Smith, The mechanical properties of the isothermal decomposition products of austenite. *Trans. Am. Soc. Met.* **28**, 380–398 (1940)
2. M. Gensamer, Static crack strength of metals; its determination and significance. *Met. Prog.*, 59–64, July 1940 (corrected diagram, *Ibid.*, August 1940, p. 181)
3. G.E. Pellissier, M.F. Hawkes, W.A. Johnson, R.F. Mehl, The derivation of an equivalent expression is described in the paper entitled “The Interlamellar Spacing of Pearlite.” *Trans. Am. Soc. Met.* **30**, 1049 (1942)
4. R.F. Mehl, The physics of hardenability, *Symposium on Hardenability of Alloy Steels*, American Society for Metals, Detroit, 1938, p. 1–65
5. C. Wells, R.F. Mehl, Rate of diffusion of carbon in austenite, in plain carbon, in nickel and manganese steels. *Trans. Am. Inst. Min. Metall. Eng. Iron Steel Div.* **140**, 279–306 (1940)
6. G.I. Taylor, The mechanism of plastic deformation of crystals. *Proc. R. Soc. A* **145**, 362–415 (1934)
7. H. Deutler, *Phys. Z.* **33**, 247–259 (1932)
8. A. Nadai, *International Association for Testing Materials*, London Conference, vol A-1-3, pp. 4–6
9. M.J. Manjoine, A. Nadai, *Proc. Am. Soc. Test. Mater.* **40**, 836 (1940)
10. W. Kauzmann, Flow of solid metals from the standpoint of the chemical rate theory. *Met. Technol. Am. Inst. Min. Metall. Eng.*, Technical Publication No. 1301, June 1941
11. G.V. Smith, The orientation relationships between austenite and its decomposition products, Thesis, Carnegie Institute of Technology, 1941 (to be published by Mehl and Smith)
12. R.F. Mehl, D.W. Smith, Orientation of Ferrite in Pearlite. *Trans. Am. Inst. Min. Metall. Eng.* **116**, 330 (1935)